energy&fuels

pubs.acs.org/EF Article

Origin and Formation of Pyrobitumen in Sinian−Cambrian Reservoirs of the Anyue Gas Field in the Sichuan Basin: Implications from Pyrolysis Experiments of Different Oil Fractions

Xing Wang, Hui Tian,* Qin Zhou, and Chunmin He

Cite This: *Energy Fuels* 2021, 35, 1165−1177 Read Online

ACCESS | Metrics & More | Article Recommendations

ABSTRACT: Plenty of pyrobitumens were found throughout the Sinian Dengying and Cambrian Longwangmiao reservoirs of the Anyue gas field in the central Sichuan Basin. However, their genetic sources and formation processes still remain less constrained due to their strong heterogeneity in carbon isotopes and contents. In this study, an oil sample collected from the Devonian bituminous sandstones in the northwestern Sichuan Basin, along with its four fractions (i.e., saturates, aromatics, resins, asphaltenes (SARA)), was pyrolyzed in sealed gold tubes to investigate the generation and evolution process of pyrobitumen. Experimental results show that the four fractions generate pyrobitumen at different thermal maturity stages during oil cracking and the pyrobitumen yields of different oil fractions follow the following order: asphaltenes > resins > aromatics > saturates. For the pyrobitumen generated from the same oil fraction, the stable carbon isotopes of pyrobitumen become only slightly heavier with increasing maturation. At the same level of thermal maturity, pyrobitumen from saturates is more enriched in ^{13}C than those from the other three oil fractions, and the maximum difference is over 2‰. Based on the experimental results, kinetic parameters for pyrobitumen generation from the four oil fractions were determined and then applied to investigate the origin and formation time of pyrobitumen in the Sinian Dengying and the Cambrian Longwangmiao reservoirs. The results show that the pyrobitumen in both the Sinian and the Cambrian reservoirs were mainly formed during the middle Jurassic to early Cretaceous. Although the pyrobitumen yields are significantly dependent on the SARA composition of oils, the change in pyrobitumen carbon isotopes is usually less than 1‰. This indicates that the carbon isotopes of pyrobitumen are mainly controlled by the initial carbon isotopes of SARA fractions that are closely related to their source rocks. Based on the carbon isotopes of pyrobitumen and potential source rocks, the precursor oils of pyrobitumen in the Cambrian Longwangmiao reservoirs are mainly derived from the Lower Cambrian Qiongzhusi source rock, while the precursor oils of pyrobitumen in the Sinian Dengying reservoirs are mixed oils sourced from both the Sinian and the Lower Cambrian source rocks.

1. INTRODUCTION

Anyue gas field is the largest carbonate monolithic gas field in China with proved resources over 1×10^{12} m^3.[1,2] Plenty of pyrobitumen was found in its reservoirs, namely, the Sinian Dengying Formation and the Cambrian Longwangmiao Formation. The presence of pyrobitumen is an indicator of in situ cracking of paleo oil pools that have suffered from severe thermal stress.[3−6] Thus, the abundance of pyrobitumen can be used to investigate the scale of paleo oil pools, which is essential for the estimation of natural gas resources in the Sinian and Cambrian reservoirs.[7,8] Earlier studies have revealed that the abundance of pyrobitumen in the Sinian and Cambrian reservoirs is governed by the paleo-uplift and the content of pyrobitumen in the core area of the uplift is higher than that in the slope region.[7,8] Wei et al.[7] also noticed that the pyrobitumen contents in the Sinian Dengying Formation are in the range of 0.1−4.0%, while they vary between 0.1 and 7.8% in the Cambrian Longwangmiao Formation.

Given the extremely low concentration and/or possible contamination of biomarkers in pyrobitumen, the correlation of pyrobitumen to its source rocks using biomarkers usually leads to high controversy.[1,9,10] For example, some scholars argued that the precursor oils of pyrobitumen in the Dengying Formation are mainly sourced from the Cambrian source rocks[9−11] while others believed that they are mainly originated from the Sinian source rocks.[12,13] As a matter of fact, the genetic origins of pyrobitumen may be effectively investigated based on their stable carbon isotopes given that they are less affected by thermal maturation than biomarkers.[14−16] The carbon isotopes of pyrobitumen in the Cambrian Longwangmiao Formation range from −35.3 to −34.6‰,[17−19] while they have a wider span varying from −36.8 to −32.8‰ in the Sinian Dengying Formation.[17,18,20,21]

Thermal maturity is the main control of pyrobitumen generation. Earlier studies have illustrated that during the thermal cracking of normal marine oils, pyrobitumen is mainly generated after the wet gas generation stage (EasyRo < 1.75%).[22,23] While normal marine oils usually have a maximum pyrobitumen yield of over 400 mg/g oil during pyrolysis,[15,23]

Received: September 29, 2020
Revised: November 25, 2020
Published: December 29, 2020

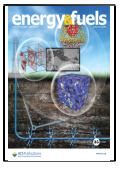

https://dx.doi.org/10.1021/acs.energyfuels.0c03263
Energy Fuels 2021, 35, 1165−1177

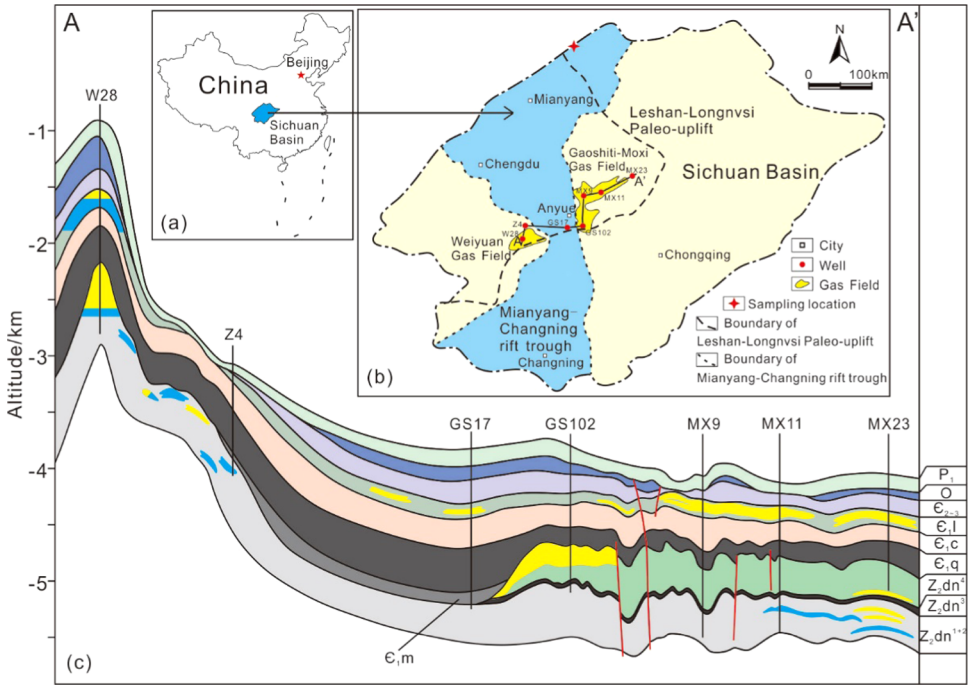

Figure 1. (a) Location of the Sichuan Basin, (b) geological map of the main structural units of the Sichuan Basin (modified with permission from Sun et al.[40]), and (c) cross section of the study area (modified with permission from Zhao et al.[8] and Zou et al.[12]).

the chemical composition of oil also determines pyrobitumen yield. For example, aromatic oils can yield more pyrobitumen than paraffinic oils,[24] and heavy oils with a high content of NSO or resin components can generate more pyrobitumen than light oils with a high content of saturates.[3] The two factors mentioned above, namely, thermal maturity and chemical composition, may also affect the carbon isotope fractionation behavior during oil cracking. Previous studies have shown that the carbon isotopes of pyrobitumen generated at higher thermal maturity levels are somewhat heavier than those generated at lower thermal maturity levels.[15] Moreover, the pyrolysis experiments by Lei et al.[25] revealed that although the initial carbon isotope of saturates is lighter than those of aromatics, resins, and asphaltenes, the carbon isotopes of pyrobitumen generated from the four isotopically different fractions are quite identical, indicating that the carbon isotopic separation between pyrobitumen and its precursor is different among the four fractions. In real geological conditions, post genetic alteration of oils such as biodegradation, gas washing, and migration fractionation also leads to variations in their fraction composition and carbon isotopes,[3,26−29] which may further complicate the carbon isotopic compositions of pyrobitumen. Therefore, knowing the specific yields and stable carbon isotopic evolution of pyrobitumen from different oil fractions would provide some new insights into the origin and formation of pyrobitumen in reservoirs.

In this study, one heavy oil sample collected from Devonian bituminous sandstones in the northwestern Sichuan Basin, along with its four fractions (i.e., saturates, aromatics, resins, asphaltenes (SARA)), was pyrolyzed in sealed gold tubes to investigate the generation and carbon isotopic evolution of pyrobitumen from the oil and its different oil fractions. The geological model for pyrobitumen generation and the stable carbon isotopes of pyrobitumen from oils with different SARA compositions were also investigated to better understand the origin and formation of pyrobitumen in the Sinian Dengying and Cambrian Longwangmiao reservoirs of the Anyue gas field in the Sichuan Basin.

2. GEOLOGICAL SETTING

The Sichuan Basin is a superimposed basin in the southwest part of China (Figure 1a). In the central and western parts of the Sichuan Basin, an inherited paleo-uplift called Leshan-Longnvsi paleo-uplift was developed during the late Ediacaran and finally shaped during the late Silurian (Figure 1b).[30−33] The Weiyuan gas field and the Anyue gas field were discovered in the eastern part of the paleo-uplift.[34−36] Recent exploration demonstrated that an approximately north-south-trending rift trough was developed during the early Cambrian and is named the Mianyang-Changning (MC) rift trough (Figure 1b).[9,19,33,35] The Weiyuan-Ziyang (WZ) Bulge and Gaoshiti-Moxi (GM) Bulge are located to the west and east of the MC rift trough, respectively (Figure 1b,c).

The Sichuan Basin has experienced multiple stages of tectonic movements (Figure 2). The Tongwan movement during the late Ediacaran resulted in two unconformities at the top of the second and the fourth members of the Dengying Formation.[32,33,36,37] From Cambrian to Silurian, the Sichuan Basin subsided continuously and received several sets of clastic and carbonate rocks. Affected by the Caledonian movement in the late Silurian, the basin was uplifted, leading to the total erosion of the Devonian to Carboniferous sequences. Entering the Permian period, the Sichuan Basin subsided again and was deeply buried during the Hercynian to early Yanshanian until it was uplifted again during the late Yanshanian to the Himalayan period (Figure 2).[13,38−40] During this period, the WZ Bulge was uplifted more intensely than the MG Bulge, finally forming the present tectonic pattern (Figure 1c).

The petroleum system of the Anyue gas field is composed of Sinian and Cambrian successions. The second and fourth members of the Dengying Formation are two sets of reservoirs, which are dominated by algal dolomite with a total thickness of

https://dx.doi.org/10.1021/acs.energyfuels.0c03263
Energy Fuels 2021, 35, 1165−1177

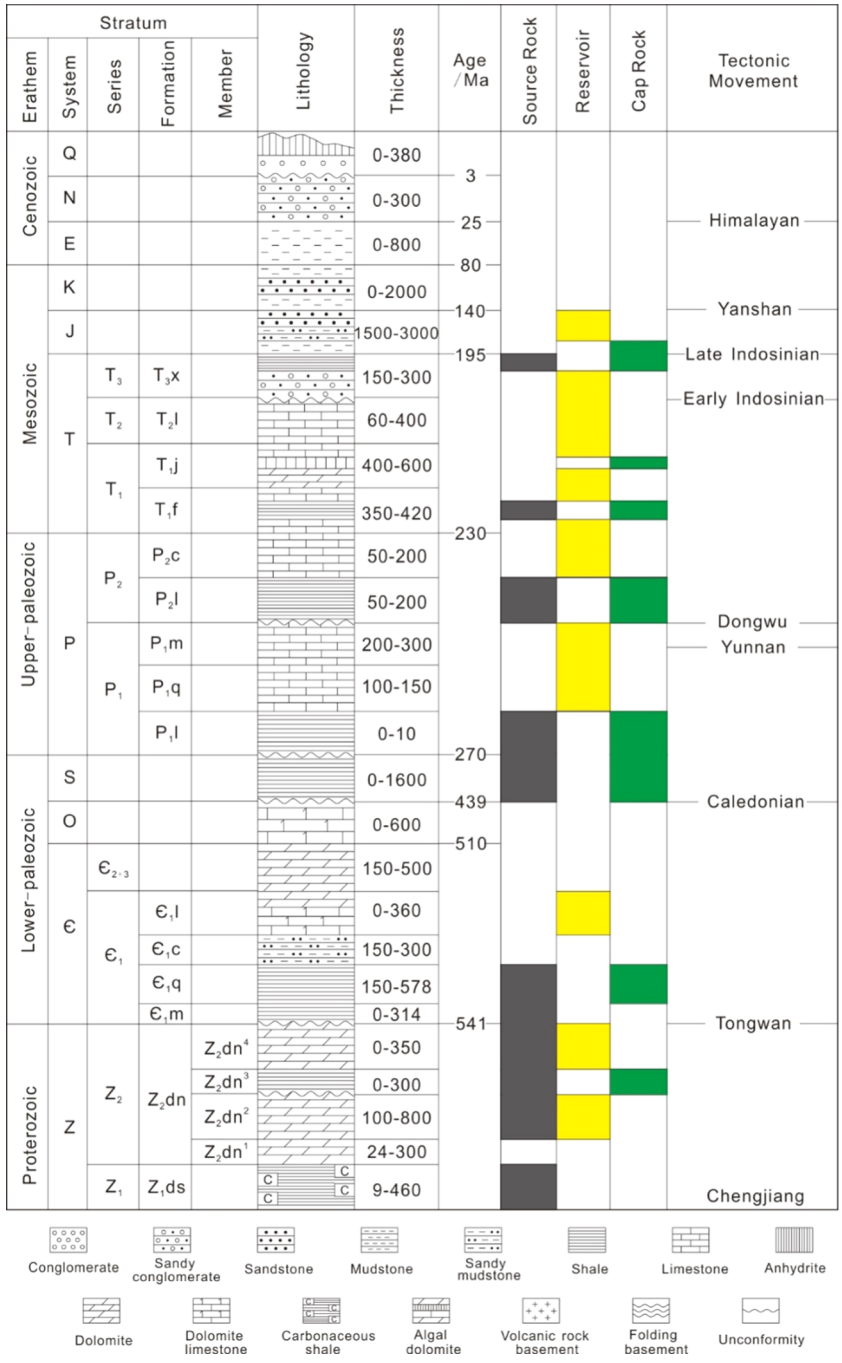

Figure 2. Generalized stratigraphy and assemblages of source rocks, reservoirs, and seals in the Gaoshiti-Moxi Bulge (modified with permission from Zhu et al.,[13] Xu et al.,[30] and Liu et al.[43]).

around 240 m.[12,20] The Cambrian Longwangmiao Formation is another main reservoir composed of dolomite with an average thickness of around 100 m.[1,31,41] The Lower Cambrian Qiongzhusi black shale is the main source rock with an average TOC value of 1.93% and a thickness of 140 m.[12] The Sinian Doushantuo Formation, the third member of the Dengying Formation, and the Cambrian Maidiping Formation are also identified as effective source rocks in this area. The Sinian Doushantuo Formation is a set of mudstones with an average TOC of 1.69% and a thickness of 11 m.[12] The third member of the Dengying Formation mainly consists of black shale with an average TOC of 0.65% and a thickness of 10−30 m.[7] The Cambrian Maidiping Formation is only distributed in the MC rift trough with a maximum thickness of over 100 m. It is composed of siliceous shale and carbonaceous mudstone with an average TOC of 1.68%.[7] Both the Sinian and Cambrian successions have equivalent vitrinite reflectance (EqVRo) values greater than 2.0%, indicating a dry gas stage.[1,6,12,42,43] The schematic assemblages of source rocks, reservoirs, and sealing rocks are presented in Figure 2.

3. SAMPLES AND EXPERIMENTS

3.1. Sample Preparation. Samples used in this study include one heavy oil sample and its SARA fractions collected from the Devonian bituminous sandstones in the northwestern Sichuan Basin (Figure 1b). Earlier studies have illustrated that

https://dx.doi.org/10.1021/acs.energyfuels.0c03263
Energy Fuels 2021, 35, 1165−1177

the heavy oil is mainly sourced from the Lower Cambrian black shales that also sourced the paleo oil pools of the present Anyue gas field.[14,44] The heavy oil sample was extracted from the bituminous sandstones with a mixture of dichloromethane and methanol (volume ratio = 93:7) in a Soxhlet extractor. The collected heavy oil sample was then dissolved in excess hexane to precipitate asphaltenes, after which the deasphalted oils were separated into saturates, aromatics, and resins using column chromatographic procedures as described by Tian et al.[45] The relative contents of saturates, aromatics, resins, and asphaltenes are 8, 22, 36, and 34%, respectively, and the low content of saturates is attributed to the severe biodegradation that preferentially removes the fraction of saturates.

3.2. Pyrolysis Experiments. The oil sample and its SARA fractions were pyrolyzed using sealed gold tubes, and the pyrolysis setups have been well described in the literature.[23,46] The experimental procedures can be summarized as follows. Approximately 5−100 mg of the sample was injected into the gold tubes with one end prewelded (length 50 mm, inner diameter 3 mm, wall thickness 0.25 mm); the gold tubes were then purged with argon for 10 min to displace the air in them, after which the other end of the gold tube was welded under argon protection. Finally, the gold tubes were placed into stainless steel autoclaves and pyrolyzed in an oven at two heating rates of 2 and 20 °C/h. The experimental temperatures were first increased from room temperature to 240 °C in 10 h and the temperature intervals were set to 20 and 24 °C for the respective runs of 2 and 20 °C/h. The experimental pressure confined to the gold tubes was maintained at around 50 MPa by pumping water into or out of the autoclaves during the pyrolysis process. At each preset temperature, the autoclave was removed from the oven and cooled in water. The EasyRo value, a proxy for thermal maturity, at each pyrolysis temperature was calculated using the method proposed by Sweeney and Burnham[47] and then they were converted to EqVRo using the method of Tang et al.[46]

3.3. Pyrolytic Products and Stable Carbon Isotopes. After the pyrolysis experiment, the gold tubes were cleaned with dichloromethane and then cut open to release the gaseous pyrolysates. The opened gold tubes were placed into 20 mL vials filled with dichloromethane and subjected to ultrasonic extraction for 2 h and left for 3 days to recover the soluble components in the gold tubes. The dichloromethane (DCM)-insoluble remnants, namely, pyrobitumen, were filtered using a glass sand core filter and collected in 8 mL vials whose mass was measured before pyrobitumen was placed. Then, the vials and pyrobitumen were dried in an oven at 120 °C for 24 h. Next, the total mass was measured and the pyrobitumen mass was calculated using the subtraction method.

Stable carbon isotopes of pyrobitumen were measured on a Finnigan Delta Plus mass spectrometer, which was connected to an elemental analyzer. The carbon in pyrobitumen was first converted to CO_2 in the elemental analyzer, and then the CO_2 was sent to the mass spectrometer for stable carbon isotope measurement. The CASEIN with a carbon isotope value of −26.98‰ made by Elemental Microanalysis Ltd. was used as an external standard, and the replicate analysis reveals an analytical error of less than 0.3‰.

4. RESULTS

4.1. Pyrobitumen Generation Characteristics. Although pyrobitumen yields of all of the four fractions increase with increasing thermal maturity, there is a remarkable difference in the generation characteristics of pyrobitumen for the different fractions (Figure 3). In general, the fraction of

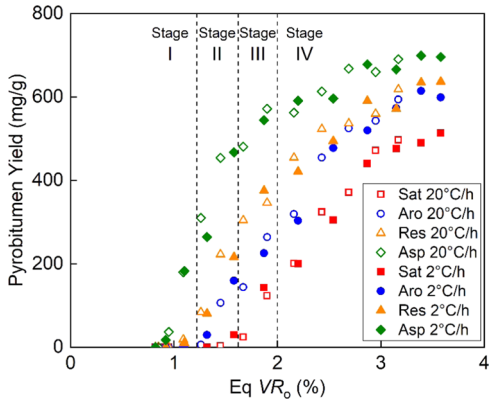

Figure 3. Change of pyrobitumen yields of the four oil fractions with thermal maturity.

asphaltenes has the highest pyrobitumen generation potential, while the fraction of saturates has the lowest pyrobitumen yields throughout the pyrolysis process. The maximum yields of pyrobitumen generated from asphaltenes and saturates were observed at 600 °C in the experimental run of 2 °C/h (EqVRo = 3.58%), and they are 699 and 513 mg/g, respectively, consistent with the results of Mort et al.[48] and Lei et al.[25] For example, Mort et al.[48] reported that approximately 72% of asphaltenes can be converted to pyrobitumen during maturation. Pyrobitumen yields of aromatics and resins are close to each other, and the maximum yields are 615 and 635 mg/g, respectively, at the highest EqVRo value of 3.58% (Figure 3). The maxima of pyrobitumen yield of aromatics in the present study are quite similar to the results of Lei et al.[25] who reported a maximum pyrobitumen yield of 631 mg/g for aromatics at the same thermal maturity level.

The pyrobitumen generation processes also differ significantly among the four fractions. To better depict these processes, four stages of oil cracking were used in this study. They are the thermally stable stage (stage I: EqVRo < 1.2%), light oil stage (stage II: EqVRo = 1.2−1.6%), condensate/wet gas stage (stage III: EqVRo = 1.6−2.0%), and the dry gas stage (stage IV: EqVRo > 2.0%).[22,25] As shown in Figure 3, the generation of pyrobitumen from saturates is negligible in stage I. At the end of stage II, there is only a small amount of pyrobitumen generated from saturates. The pyrobitumen yield of saturates at the end of stage III is about 160 mg/g, which is about 30% of the maximum pyrobitumen yield of saturates, and therefore most of the pyrobitumen from saturates (ca. 70%) is generated in stage IV, i.e., EqVRo > 2.0%. At EqVRo > 3.0%, the pyrobitumen yield of saturates remains constant, indicating almost no further gas generation from the saturates. The generation of pyrobitumen from aromatics largely begins in stage II. The pyrobitumen yield at the end of stage III is about 40% of the maximum pyrobitumen yield of aromatics observed at the highest experimental thermal maturity level and continues to increase in stage IV, though the pyrobitumen generation rate begins to slow down at EqVRo > 3.0%. Resins can generate a small amount of pyrobitumen at the end of stage I, which is followed by rapid pyrobitumen generation in stages II and III. The pyrobitumen yields of aromatics are about 42 and 60% of its maximum pyrobitumen generation potential (635 mg/g) at the end of stages II and III,

https://dx.doi.org/10.1021/acs.energyfuels.0c03263
Energy Fuels 2021, 35, 1165−1177

respectively, and continues to increase in stage IV. Asphaltenes generate pyrobitumen much earlier than the other three fractions and mainly occur from stages I to III. The pyrobitumen yield of asphaltenes is about 560 mg/g at the end of stage III, which accounts for nearly 80% of its maximum pyrobitumen generation potential (699 mg/g). At EqVRo > 3.0%, the pyrobitumen yield of asphaltenes no longer increases.

4.2. Stable Carbon Isotopes of Pyrobitumen. The initial carbon isotope of saturates is −35.2‰, a little heavier than the carbon isotopes of aromatics, resins, and asphaltenes, which are −35.6, −35.8, and −35.7‰, respectively. The saturates usually have relatively lighter carbon isotopes than the other three fractions, and the heavier carbon isotope of saturates in the present study is mainly ascribed to biodegradation that preferentially removes the isotopically light alkanes.[26,49] The carbon isotopes of pyrobitumen generated from the four oil fractions all become enriched in ^{13}C as the thermal maturity increases. For the pyrobitumen generated from any specific oil fraction, the difference among its stable carbon isotopes is usually less than 1‰ (Figure 4),

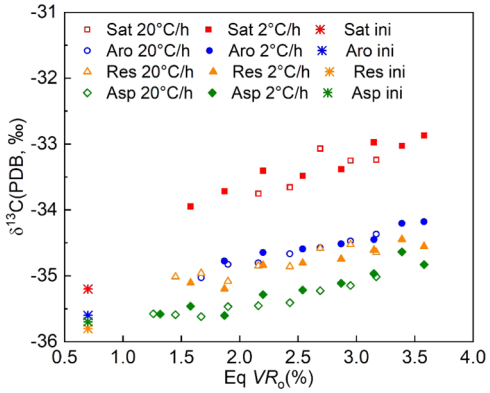

Figure 4. Stable carbon isotopes of pyrobitumen generated from four fractions at different thermal maturity levels.

which is consistent with earlier studies.[15,25] The carbon isotopes of pyrobitumen from different oil fractions vary to some extent. For example, at the same maturity level, the difference among the carbon isotopes of pyrobitumen from aromatics, resins, and asphaltenes is usually less than 1‰; however, the carbon isotopes of pyrobitumen from saturates are much heavier than those from the other three fractions, and the maximum difference is over 2‰ (Figure 4).

5. DISCUSSION

5.1. Pyrobitumen Generation. The pyrobitumen yield is closely related to the initial chemical composition of oil.[45,50,51] For example, saturates are mainly composed of alkanes and cycloalkanes that have higher H/C ratios than other fractions, and therefore they can generate more hydrogen-rich species such as methane[45] and thus lead to a relatively lower yield of hydrogen-poor pyrobitumen to meet the mass balance. Correspondingly, the asphaltenes with a lower H/C ratio have a lower hydrocarbon gas generation potential and thus would form more pyrobitumen. This can also explain why the maximum pyrobitumen yield of saturates in this study is 54 mg/g higher than that of saturates reported by Lei et al.[25] The saturates used in our study have suffered from severe biodegradation, and the alkanes that have a higher content of hydrogen have been preferentially removed.[52] This would lead to a higher yield of pyrobitumen for biodegraded saturates than normal saturates. Huc et al.[3] also illustrated that the pyrobitumen yield of biodegraded oils is much higher than that of light oils.

The different pyrobitumen generation processes may be highly related to the distinct cracking mechanisms of different oil fractions. For example, the cracking of saturates is characterized by progressive cracking of long to short saturated chains as thermal maturity increases.[23,50,53] During this process, the aromatic structure, which is the constitutional unit of pyrobitumen,[15] cannot be massively generated until thermal maturity is extremely high. Meanwhile, the cracking of asphaltenes is mainly related to demethylation from the already existing aromatic structure.[51,54] Therefore, pyrobitumen generation from asphaltenes can be much earlier than saturates. Earlier studies also suggested that the fractions of resins and asphaltenes generate pyrobitumen earlier than the fractions of saturates and aromatics during thermal maturation[25,48] and that at low thermal maturity levels, pyrobitumen generation is mainly ascribed to asphaltenes.[55]

According to the SARA composition and their respective pyrobitumen yields, the pyrobitumen yields of the oil can be calculated using the following equation

$$Y_{oil} = C_{sat} \times Y_{sat} + C_{aro} \times Y_{aro} + C_{res} \times Y_{res} + C_{asp} \times Y_{asp} \quad (1)$$

Here, Y_{oil} is the calculated pyrobitumen yield of the whole oil sample; Y_{sat}, Y_{aro}, Y_{res}, and Y_{asp} are the, respectively, measured pyrobitumen yields of the four oil fractions at the same thermal maturity. C_{sat}, C_{aro}, C_{res}, and C_{asp} are the relative abundance of saturates, aromatics, resins, and asphaltenes in the whole oil sample, which are 0.08, 0.22, 0.36, and 0.34, respectively. A comparison between the measured and the calculated pyrobitumen yields of the whole oil sample illustrates that the calculated values are quite close to the measured values (Figure 5), and therefore the individual pyrobitumen yields of

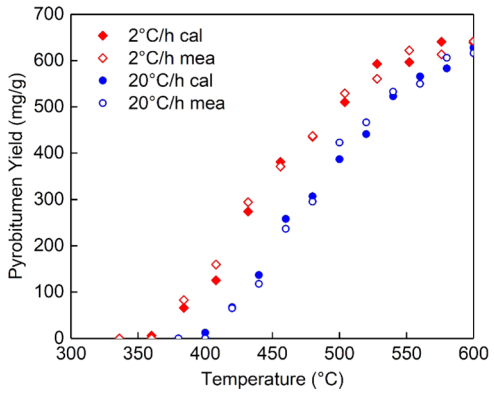

Figure 5. Plot showing the comparison of measured and calculated pyrobitumen yields of the whole oil sample at varying pyrolysis temperatures.

the four oil fractions can be used to calculate the pyrobitumen yields of the oils that have different SARA compositions, which is also reported by Lei et al.[25]

5.2. Carbon Isotopic Fractionation of Pyrobitumen. Although pyrobitumen and gaseous pyrolysates can be generated simultaneously during oil cracking, the generation mechanisms of these two products are completely different. For the gaseous pyrolysates, they can be generated either from

https://dx.doi.org/10.1021/acs.energyfuels.0c03263
Energy Fuels 2021, 35, 1165−1177

saturated chain cracking or demethylation reactions, yielding notable carbon isotopic fractionation during their generation.[23,54,56] As for pyrobitumen, which is mainly formed by aromatic condensation reactions, the carbon isotopic fractionation during thermal maturation is expected to be minor.[15,25] The pyrolysis experiment by Xiong et al.[15] has shown that as thermal maturity increases, the carbon isotopic separation between a normal marine oil and its pyrobitumen is less than 0.8‰. The influence of oil composition on pyrobitumen carbon isotopes, however, may be much more significant than thermal maturity. In our study, the pyrobitumen generated from saturates has carbon isotopes approximately 2‰ heavier than those from the other three fractions. This can be partly explained by the heavier initial carbon isotope of saturates than the other three fractions. However, the largest carbon isotope separation (approximately 2.3‰) between saturates and their pyrobitumen is much larger than the largest separation (about 1.1−1.4‰) between the other three fractions and their pyrobitumen, indicating different carbon isotope fractionations between oil fractions and their pyrobitumen. Previous studies have noted that the methane yield of different oil fractions can result in distinct carbon isotopic fractionation.[45] As the heaviest carbon isotopes of methane generated from the four oil fractions are similar and all of them are lighter than the initial carbon isotopes of their respective oil fractions,[45] the higher yield of methane leads to heavier carbon isotopes of pyrobitumen to meet the carbon isotopic balance between pyrobitumen and methane. Considering that the maximum methane yields of saturates, aromatics, resins, and asphaltenes decrease in sequence,[45] the carbon isotopes of pyrobitumen derived from them also become lighter in the same order. It is worthy to note that the maximum difference among the initial carbon isotopes of aromatics, resins, and asphaltenes is only 0.2‰; therefore, the large difference among the carbon isotopes of their pyrobitumen is most likely caused by their different methane yields. This is also consistent with the study of Machel et al.[49] who illustrated that the carbon isotopes of pyrobitumen generated from light gravity oils (containing high amounts of saturates) are 2−3‰ heavier than the initial carbon isotopes of the parent oils while the middle- or heavy-gravity oils (containing high amounts of resins and asphaltenes) generate pyrobitumen whose carbon isotopes are nearly identical to the initial carbon isotopes of oils. Although there are some amounts of ethane and CO_2 in the gaseous pyrolysates, their yields are minor at 600 °C in the experimental run of 2 °C/h, and thus their influence on the carbon isotopes of pyrobitumen can be neglected.

According to the relative proportion of pyrobitumen generated from the four fractions and their specific carbon isotopes, the carbon isotopes of pyrobitumen generated from the whole oil sample can be calculated using the following equation

$$\delta^{13}C_{oil-pyro} = M_{sat} \times \delta^{13}C_{sat-pyro} + M_{aro} \times \delta^{13}C_{aro-pyro} + M_{res} \times \delta^{13}C_{res-pyro} + M_{asp} \times \delta^{13}C_{asp-pyro} \quad (2)$$

Here, $\delta^{13}C_{oil\text{-}pyro}$ is the calculated carbon isotope of pyrobitumen generated from the whole oil sample; $\delta^{13}C_{sat\text{-}pyro}$, $\delta^{13}C_{aro\text{-}pyro}$, $\delta^{13}C_{res\text{-}pyro}$, and $\delta^{13}C_{asp\text{-}pyro}$ are the measured carbon isotopes of pyrobitumen generated from the four oil fractions; and M_{sat}, M_{aro}, M_{res}, and M_{asp} are the relative percentages of pyrobitumen generated from the four oil fractions. As illustrated in Figure 6, the calculated and measured carbon isotopes of pyrobitumen generated from the whole oil sample

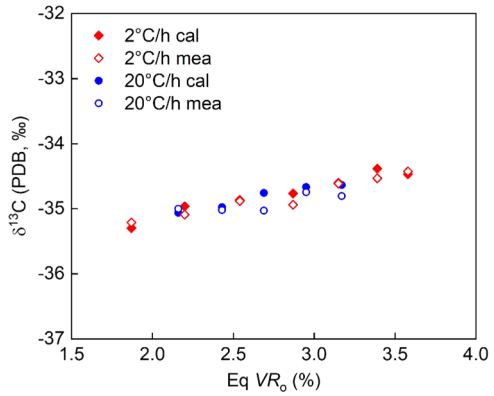

Figure 6. Plot showing the comparison of measured and calculated stable carbon isotopes of pyrobitumen generated from the whole oil sample.

are generally consistent with each other, and the maximum difference is less than 0.3‰, indicating that the method mentioned above is reliable for the determination of carbon isotopes of pyrobitumen generated from oils that have different SARA compositions.

6. KINETIC MODELING AND GEOLOGICAL IMPLICATIONS

6.1. Kinetic Modeling of Pyrobitumen Generation.

While pyrobitumen generation during pyrolysis experiments has been well depicted in our work and previous studies,[15,25] these results cannot be directly applied to real geological conditions without the establishment of a kinetic model of pyrobitumen generation.[3] Many studies have suggested that the pyrobitumen generation from oil cracking can be described by parallel first-order reactions, with a frequency factor A and activation energy E.[24,57−60] The reaction constant k obeys the Arrhenius equation

$$k = A \exp(-E/RT) \quad (3)$$

where R is the universal gas constant (J mol^{-1} K^{-1}) and T is the Kelvin temperature (K). Once kinetic parameters A and E are determined in terms of experimental results, they can be used to calculate the reaction rate of pyrobitumen generation in geological temperatures. Following this principle, Ungerer et al.[24] established a kinetic model of oil cracking that considered the generation of methane, C_2−C_5, C_6−C_{13}, and pyrobitumen under isothermal pyrolysis experiments. Behar et al.[57,58] proposed a more complicated kinetic model of oil cracking that takes into account 11 components including pyrobitumen based on the experimental results of Ungerer et al.[24] However, these kinetic models are based on a single frequency factor and activation energy, which may be inadequate to describe the complex oil cracking process in some cases.[59,61] To solve this problem, it is reasonable to regard the oil cracking process as a finite number of parallel first-order reactions, which are then described by the distributed activation energy.[62−64] Technically speaking, the distributed activation energies require distributed frequency factors. However, to simplify the calculation, a constant frequency factor for all of the parallel reactions are often used, which is adequate to describe the oil cracking process for the purpose of geological extrapola-

https://dx.doi.org/10.1021/acs.energyfuels.0c03263
Energy Fuels 2021, 35, 1165−1177

tion.[46,62−66] In this work, a constant frequency factor and distributed activation energies were used in the kinetic modeling of pyrobitumen generation. The kinetic parameters were optimized with a commercial software Kinetics 2000 based on the measured pyrobitumen yields at different pyrolysis temperatures at 2 and 20 °C/h experimental runs.

The kinetic parameters of pyrobitumen generation from different oil fractions are listed in Table 1, and the fitted results

Table 1. Kinetic Parameters for Pyrobitumen Generation from Different Oil Fractions

sample	saturates	aromatics	resins	asphaltenes
maximum yield (mg/g)	500	605	630	700
frequency factor (s^{-1})	2.35×10^{15}	8.66×10^{14}	1.49×10^{14}	7.25×10^{12}
activation energy (kcal/mol)	percent reaction	percent reaction	percent reaction	percent reaction
52				29.01
53				
54				14.43
55				21.16
56				
57				15.33
58			5	
59			21.09	
60			15.87	
61			8.98	
62		21.34		15.19
63		2.82		
64		10.11	23.82	
65				
66	25.29			
67			13.62	3.14
68		49.17		1.74
69	26.04			
70				
71			11.62	
72	35.76			
73	9.7	16.57		
74				
75				
76				
77	3.21			
total	100.00	100.01	100.00	100.00

are presented in Figure 7. Pyrobitumen generated from saturates has the highest frequency factor of 2.35×10^{15} s^{-1}, while it is only 7.25×10^{12} s^{-1} for asphaltenes. The frequency factors for pyrobitumen generated from aromatics and resins are 8.66×10^{14} and 1.49×10^{14} s^{-1}, respectively. Similarly, the activation energies for the generation of pyrobitumen from saturates (66−77 kcal/mol) are also far higher than those from asphaltenes (52−68 kcal/mol). The activation energy distributions for pyrobitumen generation from aromatics and resins are in the range of 62−73 and 58−71 kcal/mol, respectively. These kinetic parameters indicate that the saturates would generate pyrobitumen at higher thermal maturity levels than the asphaltenes.

6.2. Formation Time of Pyrobitumen in the Anyue Gas Field. The thermal history of reservoirs is required for the kinetic modeling of pyrobitumen generation in geological conditions. The GM Bulge in the central Sichuan Basin, where the Anyue gas field is located, was relatively tectonically stable during geological history.[30,40,67] The burial and thermal histories of different wells in this area are close to each other.[12,42,67] Many studies have shown that the maximum paleo-temperatures of the Sinian reservoirs in different wells are usually between 220 and 230 °C.[12,42,67,68] The difference among the thermal history of these wells is minor and thus can be neglected for the simulation of the pyrobitumen generation process. In particular, Well Moxi 9 is located in the central part of the GM Bulge and has a daily gas production of 154×10^4 m^3/day,[69] and thus the burial and thermal history of Well Moxi 9 is a reasonable representation of the study area (Figure 1). Taking this well as an example, the pyrobitumen generation process in the Sinian Dengying and the Cambrian Longwangmiao Formations at the GM Bulge was investigated. The burial history and heat flow of Well Moxi 9 established by Liu et al.[68] were utilized in this study (Figure 8). The evolution of the reservoir temperature is presented in Figure 9.

The pyrobitumen generation process from oil cracking should be calculated based on the thermal history since the oils were charged into the reservoirs rather than the whole thermal history of the reservoirs.[22] An initial temperature of 100 °C was used as the oil charging temperature (Figure 9).[70] The pyrobitumen generation from the four oil fractions in the Sinian Dengying and the Cambrian Longwangmiao reservoirs of Well Moxi 9 are presented in Figure 10. The maximum pyrobitumen yields of saturates, aromatics, resins, and asphaltenes in the Sinian Dengying reservoirs are 276, 492, 538, and 668 mg/g (Figure 10a and Table 2), while they are 175, 313, 486, and 650 mg/g for the Cambrian Longwangmiao reservoirs (Figure 10b and Table 2). Besides, the pyrobitumen generation process also differs much among the four oil fractions. In general, from early to late, the commencements of pyrobitumen generation from different oil fractions have the following order: asphaltenes, resins, aromatics, and saturates. For example, the earliest generation of pyrobitumen occurred in the early Jurassic (ca. 200 Ma) and is mainly ascribed to the asphaltenes, whereas the time for the generation of pyrobitumen from saturates only started approximately in the latest Jurassic (150 Ma).

The Sinian−Cambrian reservoirs in the Anyue gas field suffered from severe thermal stress during Cretaceous. The early charged oils had totally been cracked into natural gas and pyrobitumen. Hence, it is difficult to determine the initial SARA composition of the early charged oils.[5,6,12,68] Earlier studies have illustrated that enhanced biodegradation can result in a remarkable decrease of the saturates' content and an increase of resins and asphaltene contents, while the content of aromatics remains relatively constant.[52,71] For a normal oil, the saturates' content is about 60%, while the content of resins and asphaltenes is about 20%; for a severely biodegraded oil, the saturates' content is about 20%, while the content of resins and asphaltenes is about 60%.[52,71] In this study, we assumed three types of oils with different SARA compositions to investigate the pyrobitumen generation in reservoirs. Type I oil contains 60% of saturates, 20% of aromatics, 10% of resins, and 10% of asphaltenes; type II oil contains 40% of saturates, 20% of aromatics, 20% of resins, and 20% of asphaltenes; and type III oil contains 20% of saturates, 20% of aromatics, 30% of resins, and 30% of asphaltenes. These three types of oils can represent normal oils, moderately biodegraded oils, and severely biodegraded oils.[52,71] According to eq 1, the pyrobitumen

https://dx.doi.org/10.1021/acs.energyfuels.0c03263
Energy Fuels 2021, 35, 1165−1177

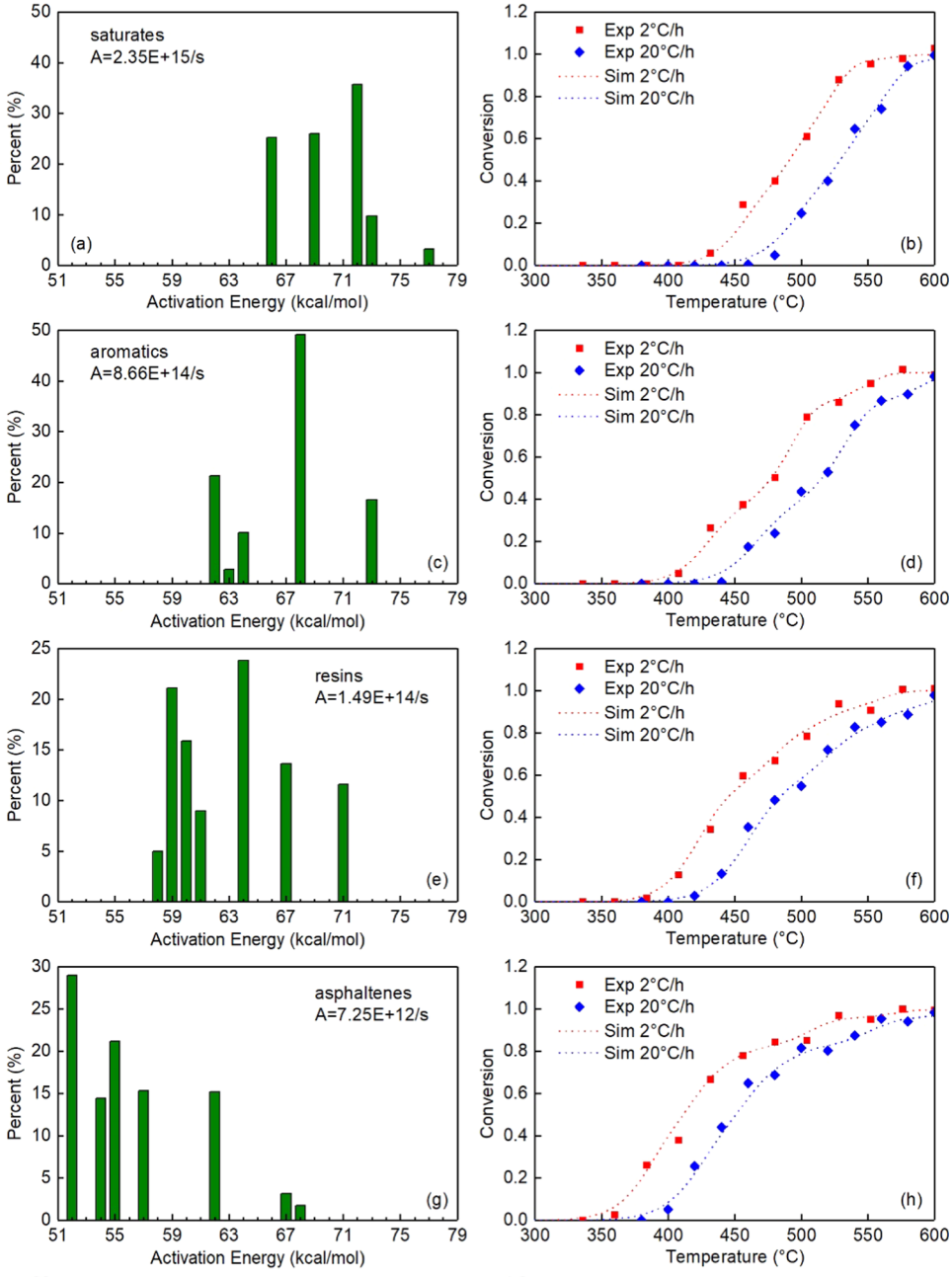

Figure 7. Kinetic parameters of pyrobitumen generation from different oil fractions (a, c, e, g) and the comparison of fitted and measured results (b, d, f, h).

yields of the three types of oils were calculated. The calculation results show that the maximum pyrobitumen yields of different types of oils increase as the saturates' content decreases and the resins and asphaltene content increases. The maximum pyrobitumen yields of the three types of oils in the Sinian Dengying reservoirs of Well Moxi 9 are 385, 450, and 515 mg/g, while they are 281, 360, and 438 mg/g, respectively, in the Cambrian Longwangmiao reservoirs (Table 2). Although there is much difference among the maximum yields of pyrobitumen generated from the three different types of oils, their main pyrobitumen generation stages are nearly the same. As illustrated in Figure 11, the pyrobitumen generation time in the Sinian reservoirs is earlier than that in the Cambrian reservoirs. However, the main pyrobitumen generation stage in both reservoirs was in the middle Jurassic to early Cretaceous. Entering the Cretaceous, pyrobitumen generation began to slow down and finally ceased in the late Cretaceous due to tectonic uplift.

6.3. Genetic Origin of Pyrobitumen in the Anyue Gas Field. The EqVRo values of pyrobitumen in the Sinian Dengying and the Cambrian Longwangmiao reservoirs at GM Bulge are about 3.5 and 3.0%, respectively.[12,42,68] At such thermal maturity levels, the carbon isotopes of pyrobitumen generated from saturates, aromatics, resins, and asphaltenes are about −32.9, −34.2, −34.4, and −34.7‰ in the Dengying reservoirs and about −33.2, −34.5, −34.6, and −35.1‰ in the Longwangmiao reservoirs, respectively (Figure 6 and Table 2). According to eq 2, the carbon isotopes of pyrobitumen generated from the three types of oils in the two reservoirs can be calculated. The calculation results show that the carbon

https://dx.doi.org/10.1021/acs.energyfuels.0c03263
Energy Fuels 2021, 35, 1165−1177

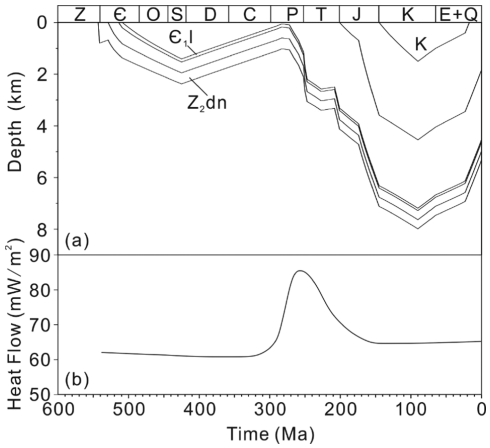

Figure 8. Burial history (a) and heat flow (b) of the Sinian Dengying and the Cambrian Longwangmiao Formations of Well Moxi 9 (adopted from Liu et al.[68]).

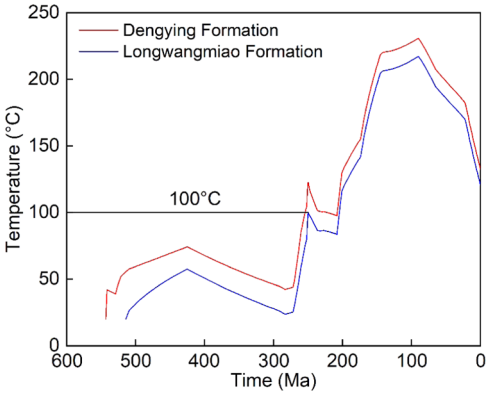

Figure 9. Plot showing the evolution of paleo-temperatures in the middle parts of the Sinian Dengying and the Cambrian Longwangmiao Formations of Well Moxi 9 based on the burial history and heat flow in Figure 8.

isotopes of pyrobitumen generated from types I, II, and III oils are −33.8, −34.1, and −34.3‰ in the Dengying reservoirs and −34.2, −34.5, and −34.7‰ in the Longwangmiao reservoirs, respectively (Figure 12 and Table 2). This illustrates that for the same genetic oils that have the same initial carbon isotopes, the difference among the carbon isotopes of their pyrobitumen at overmature stages is usually less than 1‰ even if there are

Table 2. Calculated Pyrobitumen Yields and Their Carbon Isotopes for SARA Fractions and the Three Assumed Types of Oils in the Sinian and the Cambrian Reservoirs

	pyrobitumen yield (mg/g)		δ^{13}C of pyrobitumen (‰)	
sample	Dengying	Longwangmiao	Dengying	Longwangmiao
saturates	276	175	−32.9	−33.2
aromatics	492	313	−34.2	−34.5
resins	538	486	−34.4	−34.6
asphaltenes	668	650	−34.7	−35.1
type I oil	385	281	−33.8	−34.2
type II oil	450	360	−34.1	−34.5
type III oil	515	438	−34.3	−34.7

remarkable variations in their SARA compositions and thermal maturity. In other words, the variation in carbon isotopes of pyrobitumen exceeding 1‰ may indicate that the precursor oils have distinct carbon isotopes, which may be ascribed to either their different genetic origins or the carbon isotopic heterogeneity of the same set of source rock.

Compared with the strong heterogeneity of stable carbon isotopes of kerogen in the same set of source rock due to complex variation of depositional environments and primary producers,[7,72,73] the carbon isotopes of oils in the same reservoirs are much more homogeneous.[14,74−76] Some post genetic factors, such as biodegradation, migration fractionation, and thermochemical sulfate reduction (TSR) reactions, may affect the bulk carbon isotopic compositions of oils.[21,26,77] However, even if all of these factors are considered, the difference among the carbon isotopes of oils in reservoirs from the same set of the source rock is usually less than 2‰.[75,78−80] Given that the influence of SARA compositions of oils and thermal maturity on the carbon isotopes of pyrobitumen is less than 1‰, the difference among the carbon isotopes of pyrobitumen generated from oils of the same origin is supposed to be less than 3‰.[81]

Earlier studies have revealed that the carbon isotopes of highly matured kerogen and pyrobitumen are almost identical despite various changes in the carbon isotopes of intermediate oils.[16,26] The carbon isotopes of pyrobitumen in the Cambrian Longwangmiao reservoirs range from −35.3 to −34.6‰,[17−19] plotting in the carbon isotope range of kerogen in the Lower Cambrian Qiongzhusi (from −36.0 to −31.0‰) and Maidiping (from −36.4 to −32.0‰) source rocks.[7] These values are also consistent with the calculated carbon isotopes of

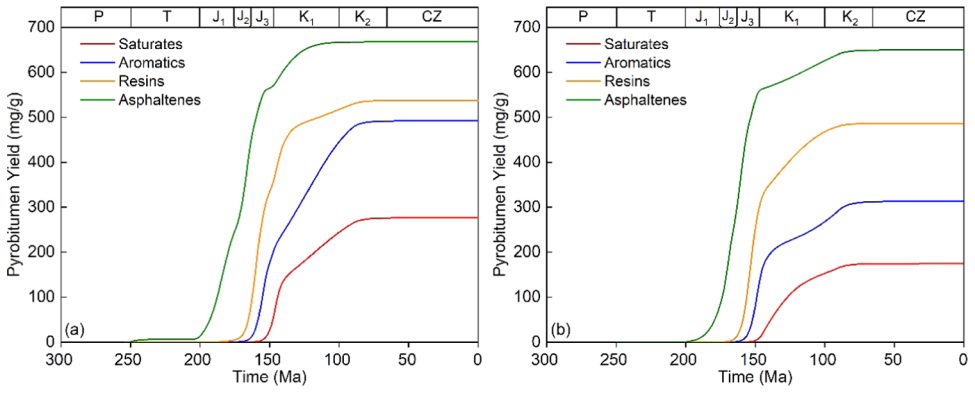

Figure 10. Pyrobitumen generation of the four oil fractions in the Sinian Dengying (a) and the Cambrian Longwangmiao (b) reservoirs in Well Moxi 9.

https://dx.doi.org/10.1021/acs.energyfuels.0c03263
Energy Fuels 2021, 35, 1165−1177

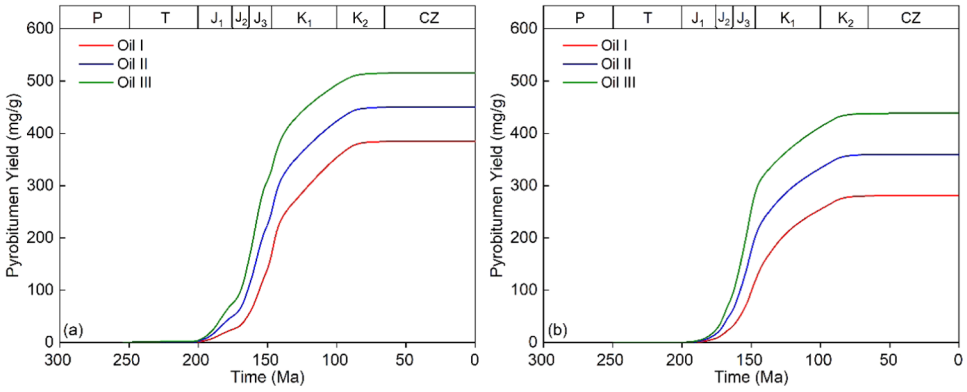

Figure 11. Pyrobitumen generation of three types of oils in the Sinian Dengying (a) and the Cambrian Longwangmiao (b) reservoirs in Well Moxi 9.

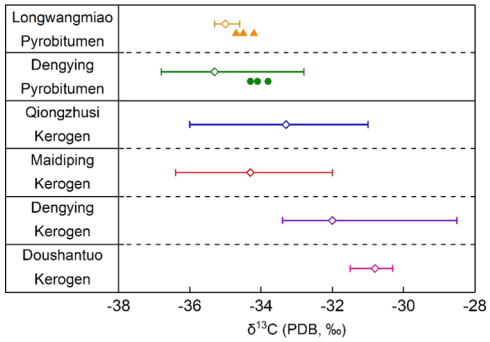

Figure 12. Carbon isotope distribution of kerogen and pyrobitumen in the Sinian and the Cambrian strata. The three solid triangles and circles are the carbon isotopes of pyrobitumen generated from the three assumed types of oils in the Longwangmiao and the Dengying reservoirs, respectively. The carbon isotope values of kerogen in the Qiongzhusi, Maidiping, Dengying, and Doushantuo source rocks are from Wei et al.[7] The carbon isotope values of pyrobitumen in the Longwangmiao reservoirs are from Gao,[17] Qin et al.,[18] and Zhang et al.[19] while those in the Dengying reservoirs are from Gao,[17] Qin et al.,[18] Shi et al.,[20] and Shuai et al.[21]

pyrobitumen generated from the assumed three types of oils sourced from the lower Cambrian source rocks (Figure 12). However, the Maidiping source rock is only distributed in the MC rift trough, and, moreover, the overlying Qiongzhusi shale also makes it difficult for the oils generated from the Maidiping source rock to migrate upward to the Longwangmiao reservoirs. Therefore, the pyrobitumen in the Longwangmiao reservoirs was mainly derived from oils sourced from the Lower Cambrian Qiongzhusi source rock.

The carbon isotopes of pyrobitumen in the Sinian Dengying reservoirs have a wide span ranging from −36.8 to −32.8‰.[17,18,20,21] These values are largely comparable with the carbon isotopes of kerogen in the Lower Cambrian Qiongzhusi and Maidiping source rocks, indicating contribution of both these source rocks to the precursor oils of pyrobitumen in the Sinian reservoirs. It is worthy to note that the lightest pyrobitumen carbon isotope (−36.8‰) in the Dengying reservoirs is much lighter than the calculated pyrobitumen carbon isotope based on the three assumed types of oils (Figure 12). This indicates that there was a precursor oil whose carbon isotope was much lighter than that of the oil used in this study (−35.4‰). As a matter of fact, Wu et al.[44] reported that the carbon isotopes of oils in the Cambrian reservoirs in the northwest part of the Sichuan Basin are as light as −36.2‰, which is 0.8‰ lighter than those of the oil (−35.4‰) used in this study. Therefore, it is inferred that there should be precursor oils with very light carbon isotopes in the Dengying reservoirs in the central Sichuan Basin similar to those in the Cambrian reservoirs in the northwestern Sichuan Basin. Similarly, the heaviest pyrobitumen carbon isotope (−32.8‰) observed in the Dengying reservoirs may be related to precursor oils that have much heavier carbon isotopic compositions than the oil used in this study. These precursor oils may be sourced from the Sinan Dengying and Doushantuo source rocks whose kerogen carbon isotopes are heavier than those of the Lower Cambrian source rocks and vary between −33.4 and −28.5‰ and from −31.5 to −30.3‰, respectively (Figure 12).[7] In summary, the wide range of carbon isotopes of pyrobitumen in the Sinian Dengying reservoirs indicates that its precursor oils have mixed genetic origins and are related to both the Lower Cambrian (Qiongzhusi and Maidiping) and the Sinian (Dengying and Doushantuo) source rocks. Geologically, the oils generated from the four abovementioned sets of source rocks can migrate either laterally or vertically to the Sinian Dengying reservoirs.[1,9,10] In addition, the organic petrology and available biomarkers in pyrobitumen reported by earlier studies also demonstrated that the Sinian source rocks have some contribution to the precursor oils of the pyrobitumen in the Sinian reservoirs.[1,82] From this perspective, the wide span of pyrobitumen carbon isotopes in the Dengying reservoirs is most likely ascribed to the mixing of oils that have different genetic origins and subsequent carbon isotopic compositions.

7. CONCLUSIONS

Remarkable differences were observed in both the generation and carbon isotopes of pyrobitumen from four oil fractions, i.e., saturates, aromatics, resins, and asphaltenes (SARA). For example, saturates generate pyrobitumen mainly in EqVRo > 2.0% with a maximum yield of 513 mg/g, while asphaltenes generate pyrobitumen mainly in EqVRo < 2.0% with a maximum yield of 699 mg/g. The largest carbon isotope separation of approximately 2.3‰ was observed between saturates and its pyrobitumen, whereas the other three fractions have relatively small carbon isotope separations of about 1.1−1.4‰ with their pyrobitumen. For our oil sample, the pyrobitumen generated from saturates is more enriched in ^{13}C than that from the other three fractions at similar thermal maturity levels.

https://dx.doi.org/10.1021/acs.energyfuels.0c03263
Energy Fuels 2021, 35, 1165−1177

Kinetic modeling of pyrobitumen generation shows that pyrobitumens in the Sinian and Cambrian reservoirs were mainly formed during the middle Jurassic to early Cretaceous. Based on the carbon isotopes of pyrobitumen in reservoirs and kerogen in potential source rocks, it is suggested that the pyrobitumen in the Cambrian Longwangmiao reservoirs originated from precursor oils mainly derived from the Qiongzhusi source rock, while the precursor oils that formed pyrobitumen in the Sinian Dengying reservoirs are most likely mixed oils from both the Sinian Dengying and Doushantuo source rocks and the Lower Cambrian Qiongzhusi and Maidiping source rocks.

AUTHOR INFORMATION

Corresponding Author

Hui Tian − *State Key Laboratory of Organic Geochemistry, Guangzhou Institute of Geochemistry, Chinese Academy of Sciences, Guangzhou 510640, China*; Phone: +86 20 85290309; Email: tianhui@gig.ac.cn

Authors

Xing Wang − *State Key Laboratory of Organic Geochemistry, Guangzhou Institute of Geochemistry, Chinese Academy of Sciences, Guangzhou 510640, China; University of Chinese Academy of Sciences, Beijing 100049, China;* orcid.org/0000-0001-9413-4365

Qin Zhou − *State Key Laboratory of Organic Geochemistry, Guangzhou Institute of Geochemistry, Chinese Academy of Sciences, Guangzhou 510640, China*

Chunmin He − *State Key Laboratory of Organic Geochemistry, Guangzhou Institute of Geochemistry, Chinese Academy of Sciences, Guangzhou 510640, China; University of Chinese Academy of Sciences, Beijing 100049, China*

Complete contact information is available at: https://pubs.acs.org/10.1021/acs.energyfuels.0c03263

Notes

The authors declare no competing financial interest.

ACKNOWLEDGMENTS

This study was jointly supported by the National Science and Technology Major Project (Grant No. 2017zx05008-002-004), the Strategic Priority Program of the Chinese Academy of Sciences (Grant No. XDA14010104), the Natural Science Foundation of China (Grant No. 41925014), and the Natural Science Foundation of Guangdong Province (Grant No. 2016A030310119). Associate Editor John Shaw and two anonymous reviewers are thanked for their constructive comments that significantly improved the whole quality and clarity of this manuscript. This is contribution No. IS-2955 from GIGCAS.

REFERENCES

(1) Wei, G.; Xie, Z.; Song, J.; Yang, W.; Wang, Z.; Li, J.; Wang, D.; Li, Z.; Xie, W. Features and origin of natural gas in the Sinian−Cambrian of central Sichuan paleo-uplift, Sichuan Basin, SW China. *Pet. Explor. Dev.* **2015**, *42*, 768−777.

(2) Zou, C.; Guo, J.; Jia, A.; Wei, Y.; Yan, H.; Jia, C.; Tang, H. Connotation of scientific development for giant gas fields in China. *Nat. Gas Ind. B* **2020**, *7*, 533−546.

(3) Huc, A. Y.; Nederlof, P.; Debarre, R.; Carpentier, B.; Boussafir, M.; Laggoun-Défarge, F.; Lenail-Chouteau, A.; Bordas-Le Floch, N. Pyrobitumen occurrence and formation in a Cambro−Ordovician sandstone reservoir, Fahud Salt Basin, North Oman. *Chem. Geol.* **2000**, *168*, 99−112.

(4) Tian, H.; Xiao, X.; Wilkins, R. W. T.; Tang, Y. New insights into the volume and pressure changes during the thermal cracking of oil to gas in reservoirs: Implications for the in-situ accumulation of gas cracked from oils. *AAPG Bull.* **2008**, *92*, 181−200.

(5) Gao, P.; Liu, G.; Lash, G. G.; Li, B.; Yan, D.; Chen, C. Occurrences and origin of reservoir solid bitumen in Sinian Dengying Formation dolomites of the Sichuan Basin, SW China. *Int. J. Coal Geol.* **2018**, *200*, 135−152.

(6) Yang, C.; Ni, Z.; Li, M.; Wang, T.; Chen, Z.; Hong, H.; Tian, X. Pyrobitumen in South China: Organic petrology, chemical composition and geological significance. *Int. J. Coal Geol.* **2018**, *188*, 51−63.

(7) Wei, G.; Wang, Z.; Li, J.; Yang, W.; Xie, Z. Characteristics of source rocks, resource potential and exploration direction of Sinian and Cambrian in Sichuan Basin. *J. Nat. Gas Geosci.* **2017**, *2*, 289−302.

(8) Zhao, W.; Zhang, S.; Ke, K.; Zeng, H.; Hu, G.; Zhang, B.; Wang, Z.; Li, Y. Origin of conventional and shale gas in Sinian-lower Paleozoic strata in the Sichuan Basin: Relayed gas generation from liquid hydrocarbon cracking. *AAPG Bull.* **2019**, *103*, 1265−1296.

(9) Wu, W.; Luo, B.; Luo, W.; Wang, W. Further discussion about the origin of natural gas in the Sinian of central Sichuan paleo-uplift, Sichuan Basin, China. *J. Nat. Gas Geosci.* **2016**, *1*, 353−359.

(10) Chen, Z.; Yang, Y.; Wang, T. G.; Cheng, B.; Li, M.; Luo, B.; Chen, Y.; Ni, Z.; Yang, C.; Chen, T.; Fang, R.; Wang, M. Dibenzothiophenes in solid bitumens: Use of molecular markers to trace paleo-oil filling orientations in the Lower Cambrian reservoir of the Moxi−Gaoshiti Bulge, Sichuan Basin, southern China. *Org. Geochem.* **2017**, *108*, 94−112.

(11) Tian, X.; Hu, G.; Li, W.; Li, X.; Su, G.; Xu, Y.; Cai, D.; Wei, H. Geochemical characteristics and significance of Sinian reservoir bitumen in Leshan-Longnvsi paleo-uplift area, Sichuan Basin. *Nat. Gas Geosci.* **2013**, *24*, 982−990.

(12) Zou, C.; Wei, G.; Xu, C.; Du, J.; Xie, Z.; Wang, Z.; Hou, L.; Yang, C.; Li, J.; Yang, W. Geochemistry of the Sinian−Cambrian gas system in the Sichuan Basin, China. *Org. Geochem.* **2014**, *74*, 13−21.

(13) Zhu, G.; Wang, T.; Xie, Z.; Xie, B.; Liu, K. Giant gas discovery in the Precambrian deeply buried reservoirs in the Sichuan Basin, China: Implications for gas exploration in old cratonic basins. *Precambrian Res.* **2015**, *262*, 45−66.

(14) Zhou, Q.; Xiao, X.; Tian, H.; Wilkins, R. W. T. Oil charge history of bitumens of differing maturities in exhumed Palaeozoic reservoir rocks at Tianjingshan, NW Sichuan Basin, southern China. *J. Pet. Geol.* **2013**, *36*, 363−382.

(15) Xiong, Y.; Jiang, W.; Wang, X.; Li, Y.; Chen, Y.; Zhang, L.; Lei, R.; Peng, Pa. Formation and evolution of solid bitumen during oil cracking. *Mar. Pet. Geol.* **2016**, *78*, 70−75.

(16) Hao, B.; Hu, S.; Huang, S.; Hu, J.; Shi, S.; Wang, K.; Liang, D. Geochemical characteristics and its significance of reservoir bitumen of Longwangmiao Formation in Moxi Area, Sichuan Basin. *Geoscience* **2016**, *30*, 614−626.

(17) Gao, P. Origin and Source of Sinian bitumen in the central Sichuan Basin. Doctoral Dissertation,China University of Petroleum: Beijing, 2016.

(18) Qin, S.; Li, F.; Zhou, Z.; Zhou, G. Geochemical characteristics of water-dissolved gases and implications on gas origin of Sinian to Cambrian reservoirs of Anyue gas field in Sichuan Basin, China. *Mar. Pet. Geol.* **2018**, *89*, 83−90.

(19) Zhang, S.; He, K.; Hu, G.; Mi, J.; Ma, Q.; Liu, K.; Tang, Y. Unique chemical and isotopic characteristics and origins of natural gases in the Paleozoic marine formations in the Sichuan Basin, SW China: Isotope fractionation of deep and high mature carbonate reservoir gases. *Mar. Pet. Geol.* **2018**, *89*, 68−82.

(20) Shi, C. H.; Cao, J.; Tan, X. C.; Luo, B.; Zeng, W.; Hong, H. T.; Huang, X.; Wang, Y. Hydrocarbon generation capability of Sinian-Lower Cambrian shale, mudstone, and carbonate rocks in the Sichuan Basin, southwestern China: Implications for contributions to the giant

Sinian Dengying natural gas accumulation. *AAPG Bull.* **2018**, *102*, 817−853.
(21) Shuai, Y.; Zhang, S.; Hu, G.; Li, W.; Wang, T.; Qin, S. Thermochemical sulphate reduction of Sinian and Cambrian natrual gases in the Gaoshiti-Moxi area, Sichuan Basin, and its enlightment for gas sources. *Acta Geol. Sin.* **2019**, *93*, 1754−1766.
(22) Tian, H.; Wang, Z.; Xiao, Z.; Li, X.; Xiao, X. Oil cracking to gases: Kinetic modeling and geological significance. *Chin. Sci. Bull.* **2006**, *51*, 2763−2770.
(23) Hill, R. J.; Tang, Y.; Kaplan, I. R. Insights into oil cracking based on laboratory experiments. *Org. Geochem.* **2003**, *34*, 1651−1672.
(24) Ungerer, P.; Behar, F.; Villalba, M.; Heum, O. R.; Audibert, A. Kinetic modelling of oil cracking. *Org. Geochem.* **1988**, *13*, 857−868.
(25) Lei, R.; Xiong, Y.; Li, Y.; Zhang, L. Main factors influencing the formation of thermogenic solid bitumen. *Org. Geochem.* **2018**, *121*, 155−160.
(26) Stahl, W. J. Compositional changes and $^{13}C/^{12}C$ fractionations during the degradation of hydrocarbons by bacteria. *Geochim. Cosmochim. Acta* **1980**, *44*, 1903−1907.
(27) Hwang, R. J.; Teerman, S. C.; Carlson, R. M. Geochemical comparison of reservoir solid bitumens with diverse origins. *Org. Geochem.* **1998**, *29*, 505−517.
(28) Kelemen, S. R.; Walters, C. C.; Kwiatek, P. J.; Freund, H.; Afeworki, M.; Sansone, M.; Lamberti, W. A.; Pottorf, R. J.; Machel, H. G.; Peters, K. E.; Bolin, T. Characterization of solid bitumens originating from thermal chemical alteration and thermochemical sulfate reduction. *Geochim. Cosmochim. Acta* **2010**, *74*, 5305−5332.
(29) Chen, Z.; Liu, G.; Cao, Z.; Gao, G.; Ren, J.; Yang, F.; Ma, W. Origin of solid bitumen and its significance to petroleum geology: A case study of Baikouquan Formation in Mahu sag of Junggar Basin. *J. China Univ. Min. Technol.* **2018**, *47*, 391−399.
(30) Xu, H.; Wei, G.; Jia, C.; Yang, W.; Zhou, T.; Xie, W.; Li, C.; Luo, B. Tectonic evolution of the Leshan-Longnüsi paleo-uplift and its control on gas accumulation in the Sinian strata, Sichuan Basin. *Pet. Explor. Dev.* **2012**, *39*, 436−446.
(31) Wei, G.; Shen, P.; Yang, w.; Zhang, J.; Jiao, G.; Xie, W.; Xie, Z. Formation conditions and exploration prospects of Sinian large gas fields, Sichuan Basin. *Pet. Explor. Dev.* **2013**, *40*, 139−149.
(32) Mei, Q.; He, D.; Wen, Z.; Li, Y.; Li, J. Geologic structure and tectonic evolution of Leshan-Longnvsi paleo-uplift in Sichuan Basin, China. *Acta Pet. Sin.* **2014**, *35*, 11−25.
(33) Duan, J.; Mei, Q.; Li, B.; Liang, Z. Sinian-early Cambrian tectonic-sedimentary evolution in Sichuan Basin. *Earth Sci.* **2019**, *44*, 738−755.
(34) Gu, Z.; Yin, J.; Yuan, M.; Bo, D.; Liang, D.; Zhang, H.; Zhang, L. Accumulation conditions and exploration directions of natural gas in deep subsalt Sinian-Cambrian System in the eastern Sichuan Basin, SW China. *Pet. Explor. Dev.* **2015**, *42*, 152−166.
(35) Wei, G.; Yang, W.; Zhang, J.; Xie, W.; Zeng, F.; Su, N.; Jin, H. The pre-Sinian rift in central Sichuan Basin and its control on hydrocarbon accumulation in the overlying strata. *Pet. Explor. Dev.* **2018**, *45*, 193−203.
(36) Yang, Y.; Yang, Y.; Yang, G.; Song, J.; Wen, L.; Deng, C.; Xia, M.; Ran, Q.; Duan, G.; Luo, B.; Xie, B. Gas accumulation conditions and key technologies for exploration & development of Sinian and Cambrian gas reservoirs in Anyue gasfield. *Pet. Res.* **2018**, *3*, 221−238.
(37) Wang, G.; Liu, S.; Liu, W.; Fan, L.; Yuan, H. Process of hydrocarbon accumulation of Sinian Dengying Formation in Gaoshiti structure, Central Sichuan, China. *J. Chengdu Univ. Technol. (Sci. Technol. Ed.)* **2014**, *41*, 684−693.
(38) Zhu, C.; Xu, M.; Shan, J.; Yuan, Y.; Zhao, Y.; Hu, S. Quantifying the denudations of major tectonic events in Sichuan basin:Constrained by the paleothermal records. *Geol. China* **2009**, *36*, 1268−1277.
(39) Yuan, Y.; Sun, D.; Li, S.; Lin, J. Caledonian erosion thickness reconstruction in the Sichuan Basin. *Chin. J. Geol.* **2013**, *48*, 581−591.
(40) Sun, W.; Liu, S.; Song, J.; Deng, B.; Wang, G.; Wu, J.; Jiao, K.; Li, J.; Ye, Y.; Li, Z.; Li, Z. The formation process and characteristics of ancient and deep carbonate petroleum reservoirs in superimposed basins: A case study of Sinian(Ediacaran) Dengying Formation in the Sichuan superimposed basin, China. *J. Chengdu Univ. Technol. (Sci. Technol. Ed.)* **2017**, *44*, 257−285.
(41) Wang, Z.; Wang, T.; Wen, L.; Jiang, H.; Zhang, B. Basic geological characteristics and accumulation conditions of Anyue gaint gas field, Sichuan basin. *China Offshore Oil Gas* **2016**, *28*, 45−52.
(42) Xu, Q.; Qiu, N.; Liu, W.; Shen, A.; Wang, X. Thermal evolution and maturation of Sinian and Cambrian source rocks in the central Sichuan Basin, Southwest China. *J. Asian Earth Sci.* **2018**, *164*, 143−158.
(43) Liu, Q.; Zhu, D.; Jin, Z.; Liu, C.; Zhang, D.; He, Z. Coupled alteration of hydrothermal fluids and thermal sulfate reduction (TSR) in ancient dolomite reservoirs − An example from Sinian Dengying Formation in Sichuan Basin, southern China. *Precambrian Res.* **2016**, *285*, 39−57.
(44) Wu, L.; Liao, Y.; Fang, Y.; Geng, A. The study on the source of the oil seeps and bitumens in the Tianjingshan structure of the northern Longmen Mountain structure of Sichuan Basin, China. *Mar. Pet. Geol.* **2012**, *37*, 147−161.
(45) Tian, H.; Xiao, X.; Wilkins, R. W. T.; Tang, Y. An experimental comparison of gas generation from three oil fractions: Implications for the chemical and stable carbon isotopic signatures of oil cracking gas. *Org. Geochem.* **2012**, *46*, 96−112.
(46) Tang, Y.; Jenden, P.; Nigrini, A.; Teerman, S. Modeling early methane generation in coal. *Energy Fuels* **1996**, *10*, 659−671.
(47) Sweeney, J. J.; Burnham, A. K. Evaluation of a simple model of vitrinite reflectance based on chemical kinetics. *AAPG Bull.* **1990**, *74*, 1559−1570.
(48) Mort, A. J.; Kowalewski, I.; Huc, A. Y.; Laggoun-Defarge, F. Investigation into tentative precursors of reservoir pyrobitumen. *Abstr. Pap. Am. Chem. Soc.* **2001**, *221*, U530.
(49) Machel, H. G.; Krouse, H. R.; Sassen, R. Products and distinguishing criteria of bacterial and thermochemical sulfate reduction. *Appl. Geochem.* **1995**, *10*, 373−389.
(50) Behar, F.; Vandenbroucke, M. Experimental Determination of the Rate Constants of the n-C25 Thermal Cracking at 120, 400, and 800 bar: Implications for High-Pressure/High-Temperature Prospects. *Energy Fuels* **1996**, *10*, 932−940.
(51) Behar, F.; Budzinski, H.; Vandenbroucke, M.; Tang, Y. Methane Generation from Oil Cracking: Kinetics of 9-Methylphenanthrene Cracking and Comparison with Other Pure Compounds and Oil Fractions. *Energy Fuels* **1999**, *13*, 471−481.
(52) Wenger, L. M.; Isaksen, G. H. Control of hydrocarbon seepage intensity on level of biodegradation in sea bottom sediments. *Org. Geochem.* **2002**, *33*, 1277−1292.
(53) McKinney, D. E.; Behar, F.; Hatcher, P. G. Reaction kinetics and n-alkane product profiles from the thermal degradation of 13C-labeled n-C25 in two dissimilar oils as determined by SIM/GC/MS. *Org. Geochem.* **1998**, *29*, 119−136.
(54) Lorant, F.; Behar, F.; Vandenbroucke, M.; McKinney, D. E.; Tang, Y. Methane Generation from Methylated Aromatics: Kinetic Study and Carbon Isotope Modeling. *Energy Fuels* **2000**, *14*, 1143−1155.
(55) Behar, F.; Pelet, R. Hydrogen-Transfer Reactions in the Thermal Cracking of Asphaltenes. *Energy Fuels* **1988**, *2*, 259−264.
(56) Tang, Y.; Perry, J. K.; Jenden, P. D.; Schoell, M. Mathematical modeling of stable carbon isotope ratios in natural gases. *Geochim. Cosmochim. Acta* **2000**, *64*, 2673−2687.
(57) Behar, F.; Ungerer, P.; Kressmann, S.; Rudkiewicz, J. Thermal evolution of crude oils in sedimentary basins: experimental simulation in a confined system and kinetic modeling. *Rev. Inst. Fr. Pet.* **1991**, *46*, 151−181.
(58) Behar, F.; Kressmann, S.; Rudkiewicz, J. L.; Vandenbroucke, M. Experimental simulation in a confined system and kinetic modelling of kerogen and oil cracking. *Org. Geochem.* **1992**, *19*, 173−189.
(59) Kuo, L.-C.; Eric Michael, G. A multicomponent oil-cracking kinetics model for modeling preservation and composition of reservoired oils. *Org. Geochem.* **1994**, *21*, 911−925.

https://dx.doi.org/10.1021/acs.energyfuels.0c03263
Energy Fuels 2021, 35, 1165−1177

(60) Behar, F.; Lorant, F.; Mazeas, L. Elaboration of a new compositional kinetic schema for oil cracking. *Org. Geochem.* **2008**, *39*, 764−782.
(61) Burnham, A. K.; Braun, R. L. Global Kinetic Analysis of Complex Materials. *Energy Fuels* **1999**, *13*, 1−22.
(62) Horsfield, B.; Schenk, H. J.; Mills, N.; Welte, D. H. An investigation of the in-reservoir conversion of oil to gas: compositional and kinetic findings from closed-system programmed-temperature pyrolysis. *Org. Geochem.* **1992**, *19*, 191−204.
(63) Schenk, H. J.; Di Primio, R.; Horsfield, B. The conversion of oil into gas in petroleum reservoirs. Part 1: Comparative kinetic investigation of gas generation from crude oils of lacustrine, marine and fluviodeltaic origin by programmed-temperature closed-system pyrolysis. *Org. Geochem.* **1997**, *26*, 467−481.
(64) Hill, R. J.; Zhang, E.; Katz, B. J.; Tang, Y. Modeling of gas generation from the Barnett Shale, Fort Worth Basin, Texas. *AAPG Bull.* **2007**, *91*, 501−521.
(65) Behar, F.; Vandenbroucke, M.; Tang, Y.; Marquis, F.; Espitalie, J. Thermal cracking of kerogen in open and closed systems: determination of kinetic parameters and stoichiometric coefficients for oil and gas generation. *Org. Geochem.* **1997**, *26*, 321−339.
(66) Waples, D. W. The kinetics of in-reservoir oil destruction and gas formation: constraints from experimental and empirical data, and from thermodynamics. *Org. Geochem.* **2000**, *31*, 553−575.
(67) Wei, G.; Yang, W.; Du, J.; Xu, C.; Zou, C.; Xie, W.; Wu, S.; Zeng, F. Tectonic features of Gaoshiti-Moxi paleo-uplift and its controls on the formation of a giant gas field, Sichuan Basin, SW China. *Pet. Explor. Dev.* **2015**, *42*, 283−292.
(68) Liu, W.; Qiu, N.; Xu, Q.; Liu, Y. Precambrian temperature and pressure system of Gaoshiti-Moxi block in the central paleo-uplift of Sichuan Basin, southwest China. *Precambrian Res.* **2018**, *313*, 91−108.
(69) Du, J.; Zou, C.; Xu, C.; He, H.; Shen, P.; Yang, Y.; Li, Y.; Wei, G.; Wang, Z.; Yang, Y. Theoretical and technical innovations in strategic discovery of a giant gas field in Cambrian Longwangmiao Formation of central Sichuan paleo-uplift, Sichuan Basin. *Pet. Explor. Dev.* **2014**, *41*, 294−305.
(70) Yuan, H.; Zhao, M.; Wang, G.; Song, J.; Liu, Y.; Fu, C.; Wang, W.; Du, W. Phases of hydrocarbon migration and accumulation in Cambrian Longwangmiao Formation of Moxi structure, Central Sichuan, China. *J. Chengdu Univ. Technol. (Sci. Technol. Ed.)* **2014**, *41*, 694−702.
(71) Jackson, R. R.; Zuo, J. Y.; Agarwal, A.; Herold, B. H.; Kumar, S.; De Santo, I.; Dumont, H.; Ayan, C.; Mullins, O. C. Mapping and Modeling Large Viscosity and Asphaltene Variations in a Reservoir Undergoing Active Biodegradation. *Soc. Pet. Eng.* **2010**, 1−20.
(72) Chen, Z.; Simoneit, B. R. T.; Wang, T. G.; Ni, Z.; Yuan, G.; Chang, X. Molecular markers, carbon isotopes, and rare earth elements of highly mature reservoir pyrobitumens from Sichuan Basin, southwestern China: Implications for PreCambrian-Lower Cambrian petroleum systems. *Precambrian Res.* **2018**, *317*, 33−56.
(73) Fang, X.; Wu, L.; Geng, A.; Deng, Q. Formation and evolution of the Ediacaran to Lower Cambrian black shales in the Yangtze Platform, South China. *Palaeogeogr., Palaeoclimatol., Palaeoecol.* **2019**, *527*, 87−102.
(74) Chen, Z.; Ma, F.; Xiao, G.; Zhang, Y.; Gao, Y.; Wang, X.; Han, C. Oil-sources rock correlation of Baiyingebi Formation in Hari sag, Yingen-Ejinaqi Basin. *Oil Gas Geol.* **2019**, *40*, 900−916.
(75) Chung, H. M.; Rooney, M. A.; Toon, M. B.; Claypool, G. E. Carbon Isotope Composition of Marine Crude Oils. *AAPG Bull.* **1992**, *76*, 1000−1007.
(76) Wu, X.; Cao, Z.; Lu, Q.; Hong, C. Genetic types and sources of Cretaceous crude oil in Shunbei area, Tarim Basin. *Pet. Geol. Exp.* **2020**, *42*, 255−262.
(77) Peters, K. E.; Moldowan, J. M. Effects of source, thermal maturity, and biodegradation on the distribution and isomerization of homohopanes in petroleum. *Org. Geochem.* **1991**, *17*, 47−61.
(78) Sofer, Z. Stable Carbon Isotope Compositions of Crude Oils: Application to Source Depositional Environments and Petroleum Alteration. *AAPG Bull.* **1984**, *68*, 31−49.
(79) Shi, J.; Li, J.; Li, Z.; Hao, A. Geochemical characteristics and origin of the deep Cambrian oil and gas in the Tazhong Uplift, Tarim Basin. *Oil Gas Geol.* **2017**, *38*, 302−310.
(80) Liu, H.; Li, H.; Xiang, H.; Wang, X.; Du, S. Geochemistry, genesis and distributions of crude oilsin the Fukang Fault zones and their periphery in Jungur Basin. *Nat. Gas Geosci.* **2020**, *31*, 258−267.
(81) Zhao, M.; Zhang, S.; Zhao, L.; Da, J. Geochemical features and genesis of the natural gas and bitumen in paleo-oil reservoirs of Nanpanjiang Basin, China. *Sci. China, Ser. D: Earth Sci.* **2007**, *50*, 689−701.
(82) Liu, D.; Li, J.; Xie, Z.; Guo, J.; Hao, A. Origin and significance of Sinian original and coexist bitumen of central Sichuan Basin. *Pet. Geol. Exp.* **2014**, *36*, 218−223.

https://dx.doi.org/10.1021/acs.energyfuels.0c03263
Energy Fuels 2021, 35, 1165−1177